Nig. J. of Pure & Appl. Physics Vol. 2 No. 1 pages 28 – 33, 2003

# PRELIMINARY STUDY OF THE TRENDS IN MONOVACANCY FORMATION ENERGY OF METALS

A. M. Ukpong and I. A. Fuwape,
Department of Physics, Federal University of Technology, Akure, P. M. B. 704, Akure, Nigeria.

**Abstract.** The monovacancy formation energy has been calculated for the various metal series of the periodic table within the local density approximation of the density functional theory. The calculations were done using the full potential Kohn-Korringa-Rostoker (FP-KKR) approach and the *ab initio* relaxed core pseudopotential in combination with the supercell approach. The results obtained from these calculations are in good agreement with experimental values obtained from positron annihilation rates. An interpretation of the trends in the variation of the formation energies through these metal series is also presented.

## 1. INTRODUCTION

The existence of defects in metals is of considerable technological interest because metals with defects show remarkable mechanical, thermal and electronic properties. For instance, [1 – 5] assert that defects control plasticity in metals and also give rise to energy levels in the band gap of metals. Also in his recent study, [2] investigated the contributions from inter-vacancy interactions to the electrical activity in semiconductors. They concluded that at equilibrium conditions, the defect concentration at faults is high as a result of the low formation energy suggesting that at non equilibrium conditions, the faults act as sinks to point defects.

As a result, considerable efforts have been directed towards the study of the formation energies of vacancies and their effect on the bulk properties of metals. The use of positron annihilation measurements to determine the monovacancy formation energy in metals has been adequately documented [6,7]. On the other hand, a wide range of computational techniques has been used to obtain a good insight into the vacancy formation energy of some metals to varying degrees of success. For instance, [8] carried out studies on the self-consistent electronic structure of a vacancy in aluminium using the reciprocal lattice method and obtained vacancy formation energy 2.9 times the experimental value.

Recently, [9] carried out first-principles study of vacancy formation energy in transition and noble metals using Green function method. They asserted that the variation of the vacancy formation energy through the transition metal series is similar to the cases of cohesive surface energies that are usually explained using Friedel's rectangular state-density approximation. Also, [10] used cluster method to carry out *ab initio* investigation of point defects in bulk silicon and germanium. They concluded that the results of the calculations are sensitive to structural effects such as the lattice constant at which computations are carried out. Similarly, [11] also carried out first principles study of vacancy formation and migration energies in tantalum using the plane-wave pseudopotential method in the density functional theory. They emphasized that including structural relaxations in the vacancy calculations leads to a reduction of the formation energy by as much as 14%. They also suggested that this decrease depends on crystal structure. Also, [12] evaluated the formation energies of vacancies and adatom-vacancy pair using the embedded-atom method (EAM) and the modified embedded- atom method (MEAM) for some metals. They concluded that including structural relaxations and crystal structure effect yields underestimated vacancy formation energies for metals. Furthermore, [13] used plane wave pseudopotential of uranium in the Troullier-Martins form to study the uranium and oxygen point defects in uranium oxide using the supercell method. They interpreted the results of vacancy calculation based on the point defect model (PDM), and noted that the validity of the PDM in obtaining a satisfactory description of the population of defects in uranium dioxide is doubtful.

In spite of all these however, no self-consistent study of the trends in the variation of the monovacancy formation energy along the various metal series of the periodic table has been carried out so far. Instead, [14,15] suggest a wide range of theoretical predictions of vacancy formation energy based on the theories of bonding in metals. Consequently, this paper presents the results of a self-consistent calculation of the monovacancy formation energy in metals using the full potential Kohn-Korriger-Rostoker (FP-KKR) approach and the *ab initio* relaxed core pseudopotential. We also present a preliminary interpretation of the trends in the formation energies calculated using these approaches.

---

*Nig. J. Pure Appl. Phys (2003) Vol.2 pp 28 - 33. Printed in Nigeria ISSN 1596-0862. Email :njpap@futa.edu.ng For rights of reproduction and web access, contact African Jounals Online, UK. www.inaps.ajol.*

## 2. COMPUTATIONAL PROCEDURE

### 2.1 *Total Energy*

The electronic states and total energies were calculated based on the density functional theory (DFT) of the local density approximation (LDA) using the full-potential Korringer-Kohn-Rostoker (FP-KKR) results proposed by [16]. Also, the total energy was calculated for a system of $N$ interacting electrons in a given ionic potential [17 – 19] as

$$E(n) = T_s[n(r)] + \int V_{ion}(r)n(r)dr + \frac{1}{2}\int \frac{n(r)n(r')drdr'}{|r-r'|} + E_{XC}[n(r)] \tag{1}$$

$T_s[n(r)]$ is the exact kinetic energy of the non interacting electron gas in its ground state with density distribution n(r), the second term gives the ionic potential, which is directly dependent on the pseudopotential [20] as,

$$V_{ion}(r) = \sum_{l}\sum_{\alpha}\phi_b(r+l) \tag{2}$$

$\phi_b$ represents the pseudopotential. The summations are over all lattice vectors $l$ in the infinite crystal and number of atoms α in the unit cell.

The expression adopted for the bare-ion pseudopotential is the Fourier transform of the local form of the relaxed core pseudopotential [21], generated in the *ab initio* approach is enumerated and expressed using [22] as

$$\phi_b(q) = -\frac{4\pi Ze^2}{\Omega q^2}\cos\left(\frac{qr_s}{2}\right)\exp\left(-\frac{qr_s}{2}\right) \tag{3}$$

In this case, $Z$, $e$, $r_s$, and $q$ represent the valence, the electronic charge, the radius of the Wigner-Seitz primitive cell and momentum transfer vector respectively. When the local form of this potential is treated as a perturbation and the corresponding shifts in valence electron energy are obtained from the stationary state perturbation theory, the eigenvalues are found to be identical with the free atom eigenvalues in line with the free electron gas approximation.

The third and the last terms of eqn. (1) denote the classical Coulomb energy and the exchange-correlation energy respectively. However, since the exact form of the exchange-correlation energy is not known exactly, we therefore adopt the approximate exchange-correlation functional of [23] expressed as,

$$V_{XC} = V_{XC}[n(r)] \tag{4}$$

In the Kohn-Sham formalism, the ground state electron density is the density that minimizes the total energy E[n]. This is given by

$$\frac{\delta E[n]}{\delta n(r)} = 0 \tag{5}$$

subject to the condition of

$$\int n(r)dr = N \tag{6}$$

In atomic units, setting $\hbar = m = 1$, and replacing the net potential by a self-consistent field potential in the one-body Schroedinger equation leads to the exact single particle Kohn-Sham equations which were solved self-consistently.

Furthermore, the self-consistent results of the FP-KKR calculations for metals were used within the supercell approach to evaluate the electronic states and total energy. Therefore, we do not require an arbitrary cut off kinetic energy since all energy terms are simulated in terms of the stationary state perturbation theory by treating the pseudopotential and the full potential as perturbations respectively.

### 2.2 *Defect Calculation*

In calculating the supercell energy, we adopted the approach of. [8] as modified by [20]. The computation of monovacancy properties is based on the supercell approach as enumerated by [3,14,15]. In this approach, a bulk crystal is represented by a supercell geometry in which all but one lattice sites are occupied by atoms to represent the metal-monovacancy system. Furthermore, since the total energy convergence in defect calculations are known to depend on supercell size, and in order to make the effects of inter vacancy interactions negligible, we select a large supercell of size N = 54 lattice sites, to ensure a rapid convergence of the supercell energies to the bulk energies.

The supercell energies were first obtained using the results of the FP-KKR calculation for metals and then with the relaxed core pseudopotential. The energy of formation of vacancies at constant pressure in a bulk crystal system of total energy $E(n)$, containing $N$ atoms and $n_v$ vacancies occupying $N + n_v$ lattice sites in a crystal volume $\Omega$ has been evaluated by [8,9]

$$E^f_{1_v} = E[N-1,1;\Omega(N-1,1;0)] - \frac{N-1}{N}E(N,0;N\Omega_0) \tag{7}$$

where $\Omega_0$ is the bulk equilibrium atomic volume and $\Omega(N,n_v,P)$ is the equilibrium volume of the system of $N$ atoms and $n_v$ vacancies at pressure $P$. The first and second terms of eqn. (7) represent the bulk energy of the supercell with one vacancy and the total energy of the bulk perfect crystal obtained from the self-consistent calculations respectively.

## 3. RESULTS AND DISCUSSIONS

The results of the monovacancy formation energy calculated using the full-potential Kohn-

Korringa-Rostoker (FP-KKR) approach and the *ab initio* relaxed core pseudopotential (PP) are presented as shown in Tables (1-6). A plot of the monovacancy formation energy for the metal series considered is presented in Figs. (1-6). It is observed in figure 1 that monovacancy formation energies of alkali metals calculated using the FP-KKR method are higher than those obtained using the relaxed core pseudopotential. This trend persists for the alkaline earths other than calcium and zinc as observed in figure 2. However, since there are no experimental values for most of the metals considered, we compare our results with those of other theories. It is noted that the results obtained for transition metals show that the relaxed core pseudopotential over estimates the monovacancy formation energy.

We ascribe this trend to the large atomic and ionic radii observed for the transition metal series, which causes a depression in the transition metal pseudopotential and further confirms the volume and structural dependence of the calculated energies. Specifically, the results obtained in this study for indium using these approaches show a strong correspondence with the experimental value of [7].

Table 1: The monovacancy formation energy of alkali metals obtained using a model potential and the FP-KKR method.

| Element | Model Calculation (eV) | FP-KKR calculations (eV) |
|---|---|---|
| Li | 1.56 | 1.48 |
| Na | 1.96 | 1.88 |
| K | 2.70 | 2.62 |
| Cs | 2.89 | 2.63 |

Table 2: The monovacancy formation energy of alkaline–earth metals obtained using a model potential and the FP-KKR method.

| Element | Model Calculation (eV) | FP-KKR calculations (eV) |
|---|---|---|
| Ca | 0.30 | 0.23 |
| Zn | 0.68 | 0.54 |
| Mg | 0.93 | 1.33 |
| Ba | 0.73 | 0.88 |

Table 3: The monovacancy formation energy of 3*d*- transition metals obtained using a model potential (PP) and the FP-KKR method, *a* are results of [9] for fcc metals, *b* are results of previous full potential (FP) calculations for fcc metals. Results quoted in parenthesis are results for bcc metals.

| Element | PP (eV) | FP-KKR (eV) | Other Theories | |
|---|---|---|---|---|
| | | | /a/ | /b/ |
| Sc | 1.35 | 1.48 | 1.52 (1.21) | 1.85 |
| Ti | 1.67 | 1.84 | 1.67 (1.63) | 2.13 |
| V | 1.25 | 1.38 | 2.03 (2.20) | (3.06) |
| Cr | 1.97 | 2.14 | 2.12 (2.70) | (2.86) |
| Mn | 1.06 | 1.33 | 2.51 (1.51) | |
| Fe | 1.52 | 1.94 | 2.65 (1.30) | |
| Co | 1.40 | 1.52 | 2.15 (1.52) | 2.18 |
| Ni | 1.42 | 1.66 | 1.67 (1.65) | 1.76, (1.77) |
| Cu | 1.34 | 1.38 | 1.33 (1.23) | 1.41, (1.33) |

Table 4: The monovacancy formation energy of 4*d*- transition metals obtained using a model potential PP and the (FP-KKR) method.

| Element | PP (eV) | FP-KKR (eV) | Other Theories | |
|---|---|---|---|---|
| | | | /a/ | /b/ |
| Y | 1.56 | 1.48 | 1.51 (1.12) | 1.74 |
| Zr | 1.96 | 1.88 | 1.70 (1.68) | 1.77 |
| Nb | 2.70 | 2.62 | 2.00 (2.32) | (2.92) |
| Mo | 2.89 | 2.63 | 2.17 (2.50) | (3.13,2.90) |
| Tc | 2.46 | 2.33 | 2.46 (1.45) | 2.56 |
| Ag | 1.23 | 1.03 | 0.96 (0.87) | (1.20,1.24,1.06 |

Table 5: The monovacancy formation energy of 5*d*- transition metals obtained using a model potential and the FP-KKR method, *c* is the result of the Full Potential Linear Muffin Tin Orbital (FP-LMTO) method, *d* is the result obtained by [14], *e* is the result obtained by [11]

| Element | PP (eV) | FP-KKR (eV) | Other Theories | | | | Experiment |
|---|---|---|---|---|---|---|---|
| | | | /c/ | /d/ | /e/ | /f/ | (eV) |
| La | 0.94 | 0.88 | | | | 1.54 (1.08) | |
| Hf | 2.35 | 2.28 | | | | 1.69 (1.56) | |
| Ta | 3.14 | 2.97 | | | 3.00 | 2.42 (2.41) | 3.10 |
| W | 3.36 | 3.24 | 3.27 | 3.44 | 3.68 | 2.49 (3.04) | 3.61±0.2, 3.51±0.2 |
| Re | 3.22 | 3.06 | | | | 2.89 (1.27) | |
| Au | 1.09 | 0.95 | | | | 0.77 (0.82) | |

Table 6: The monovacancy formation energy of some polyvalent metals obtained using a model potential and the FP-KKR method; *g* is the result of Suzuki et al. [7].

| Element | Model Calculation (eV) | FP-KKR calculations (eV) | Other Theories /g/ |
|---|---|---|---|
| Al | 0.89 | 0.92 | |
| Ga | 0.30 | 0.42 | |
| In | 0.43 | 0.61 | 0.48±0.02 |
| Tl | 0.58 | 0.66 | |
| Re | 3.22 | 3.06 | |
| Au | 1.09 | 0.95 | |

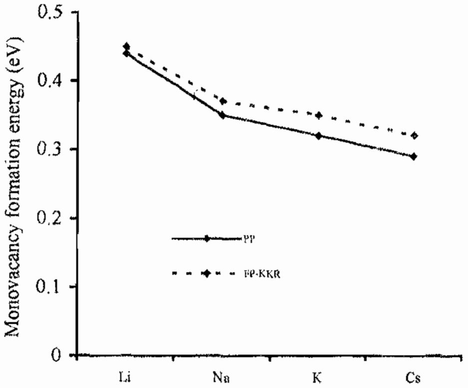

Fig 1: The monovacancy formation energy of alkali metals calculated using the relaxed core pseudopotential and the FP-KKR method.

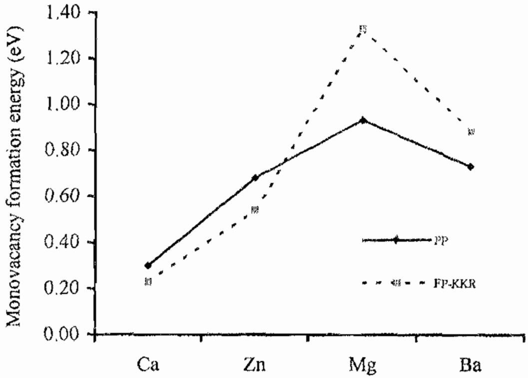

Fig 2: The monovacancy formation energy for some alkaline earth metals calculated using the relaxed core pseudopotential and the FP-KKR method.

It is further noted that the observed trend in these metals (Figs. 1-6) are similar to that of the cohesive energy, which is usually explained in terms of the Friedel's rectangular state-density model in the tight binding approximation [24]. Apart from the alkali metals, the Friedel model when applied in calculating the monovacancy formation energy yields a maximum at the centre of the rare earth metals and transition metal series but with large discrepancies in calculated values. Therefore, since the cohesive energy varies parabolically with the *d* occupation number, we speculate that an implicit relationship exists between the vacancy formation energy, the cohesive energy and the spin orbit interaction for metals.

Consequently, we assert that the irregularities in the monovacancy formation energy observed near the centre of the various transition metal series could have arisen from spin polarizations associated with Hund's rule. This effect apparently causes an extremum in the monovacancy formation energy obtained at the centre of the transition metal series. Furthermore, we ascribe this observed trend to the gradual lessening in the difference in localization between the *d* electrons and the *s* electrons observed through the transition metal series. Therefore, in line with [25], we note that in the left end of the transition metal series, and as we move down the transition metal series, the 3*d*, 4*d* and 5*d* states are much more like the *s* and *p* valence states and therefore contributes to bonding.

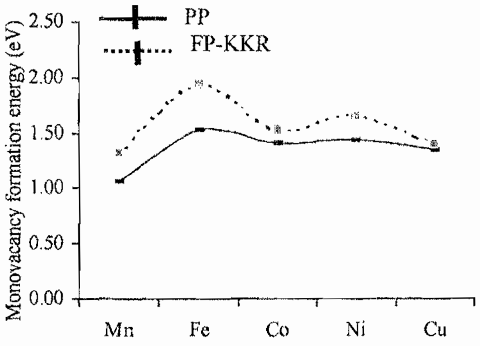

Fig 3: The monovacancy formation energy for 3d transition metals calculated using the relaxed core pseudop[otential and the FP-KKR method.

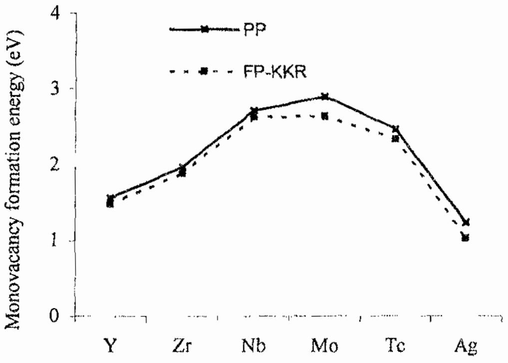

Fig 4: The monovacancy formation energy for 4d transition metals calculated using the relaxed core pseudopotential and FP-KKR method.

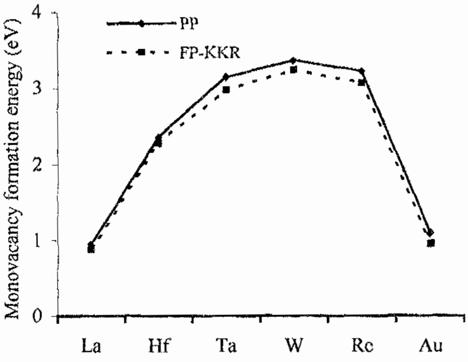

Fig 5: The monovacancy formation energy for 5*d* transition metals calculated using the relaxed core pseudopotential and FP-KKR method.

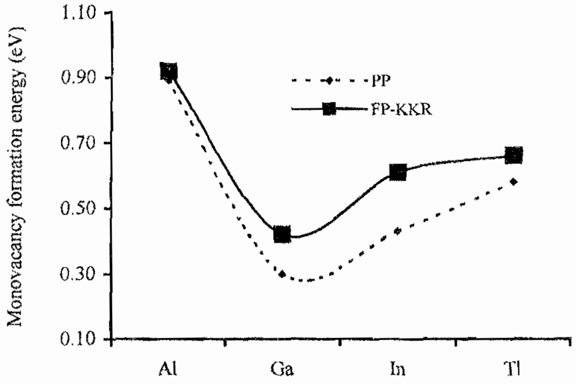

Fig 6: The monovacancy formation energy for trivalent metals calculated using the relaxed core pseudopotential and FP-KKR method.

However, we note that in the alkali, alkaline earth metals and the trivalent metals, the effect of spin orbit interaction is not very large because of the relatively small atomic cores associated with metals of these groups. Therefore, this effect is not very pronounced in these groups and consequently, a minimum is observed in the monovacancy formation energy at the middle of these series in line with experimental results.

## 4. CONCLUSION

A preliminary study of the trends in the monovacancy formation energy of metals has been presented. The agreement of our results with available experimental values is as good as other theories, further confirming the validity of the relaxed core pseudopotential. We state in conclusion, that the trends show that structural effects such as equilibrium atomic volume, type of crystal structure, *d* occupation number and lattice parameter contribute significantly to the vacancy formation energy in metals. As a result, we further speculate that spin orbit interaction influences the formation energy implicitly through the pseudopotential.

## REFERENCES

1. Kittel, C., (1976). Introduction to Solid State Physics, 5th Edtion, John Wiley and Sons: 537pp.
2. Antonelli, A., Justo, J. F. and Fazzio, A., (1999) Point defect interactions with extended defects in semiconductors. *Phys. Rev. B*, Vol. 60, No. 7: 4711-4714.
3. Aradi, B., Gali, A., Deák, P., Lowther, J. E., Son, N. T., Janzén, E., and Choyke, W. J., (2001). Ab initio density functional supercell calculation of Hydrogen defects in cubic SiC. *Phys. Rev. B*, Vol. 63: 245202(1)-245202(19).
4. Chua, S. J., Choi, H.W., Zhang, J. and Li, P., (2001). Vacancy effects on plasma induced damage to n-type GaN. *Phys. Rev. B*, Vol. 64: 205302(4).
5. Foster, A. S., Sulimov, B. V., Lopez Gejo, F., Shluger, A. L., and Nieminen, R. M., (2001). Structure and electrical levels of point defects

in monoclinic zirconia. *Phys. Rev. B*, Vol. 64: 224108(6).

6. Erhrhat, P., Jung, P., Schultz, H., and Ullmaier, H., (1991). Atomic Defects in Solids:, In H. Ullmaier, Landolt-Börnstein (Editor), New Series, Group III, Vol. 25, Springer-Verlag, Berlin.
7. Suzuki, N., Yasuyoshi, N., Yoshiko, I., Akira, G., Yasushige, Y., and Toshino, Hyodo.,(2001). Vacancy formation energy for Indium determined by a positron annihilation technique. *Phys. Rev. B*, Vol. 63: 180101(R).
8. Chakraborty, B., Siegel, R. W., and Picket, W. E., (1981). Self-consistent electronic structure of a vacancy in Aluminium, *Phys. Rev. B*, Vol. 24: 5445(15).
9. Korzhavyi, P. A., Abrikosov, I. A., Johannson, B., Ruban, A.V., and Skriver, H. L., (1999). First principles calculations of the vacancy formation energy in transition and noble metals. *Phys. Rev. B*, Vol. 59, No. 18: 11693-11703.
10. Őğüt, S. and Chelikowsky., J. R., (2001). *Ab initio* investigation of point defects in bulk Si and Ge using a cluster method. *Phys. Rev. B*, Vol. 64: 245206 (1) – 245206(11).
11. Satta, A., Williame, F., and Gironcoli, S., (1999). First principles study of vacancy formation and migration energies in tantalum. *Phys. Rev. B*, Vol. 60, No 10: 7001-7005.
12. Devyatko, Y. N., Rogozhkin, S.V. and Fadeev, A. V., (2001). Point defects at low index surfaces of fcc metals: Formation energy of vacancies and adatom-vacancy pairs. *Phys. Rev. B*, Vol. 64: 193401(1) – (3).
13. Cocombette, J.P. Jollet, F. Thien Nga, L., and Petit, T., (2001). Plane wave pseudopotential study of point defects in uranium dioxide. *Phys. Rev. B*, Vol. 64: 104107 (1) – (12).
14. Satta, A., Williame, F., and Gironcoli, S., (1998). Vacancy self-diffusion parameters in tungsten: Finite electron-temperature LDA calculations. *Phys. Rev. B*, Vol. 57, No 18: 11184 - 11192.
15. Le Bacq, O., Williame, F., and Pasturel, A., (1999). Unrelaxed vacancy formation energies in group IV elements by the full potential linear muffin tin orbital method: invariance with crystal structure. *Phys. Rev. B*, Vol. 59, No. 13: 8508-8515.
16. Asato, M., Settels, A., Hoshino, T., Asada, T., Blügel, S., Zeller, R, and Dederichs, P. H. (1999). Full-potential KKR calculations for metals and semiconductors. *Phys. Rev. B*, Vol. 60, No 8: 5202-5210.
17. Hohenberg, P. and Kohn, W. (1964), Inhomogeneous electron gas, *Phys. Rev. B*, Vol. 136: 864.
18. Kohn, W. and Sham, L. J. (1965). Self consistent equations including exchange and correlation effect, *Phys. Rev.* Vol. 140, A1133.
19. Kohn, W. (1999). Nobel Lecture: Electronic Structure of Matter-Wave Functions and Density Functionals, *Rev. Mod. Phys.*, Vol. 71, No. 5, pp 1258-1265.
20. Jarvis, M. R., Whito, I. D., Godby, R. W., and Payne, M. C., (1997). Supercell Technique for total energy calculations of finite charged and polar systems. *Phys. Rev. B*, Vol. 56: 14972.
21. Ukpong, A. M. and Fuwape, I. A., (2001). *Ab initio* relaxed core pseudopotential. *Journal of Applied Sciences and Humanities* (in press).
22. Vackar, J., Hyt'ha, M., and Simunek, A. (1998). All-electron pseudopotential. *Phys. Rev. B*, Vol. 58: 12713-12715.
23. Gunnarsson, O. and Lundqvist, B. I. (1976). Exchange and correlation in atoms, molecules and solids by spin density formalism, *Phys. Rev. B*, Vol. 13: 4274
24. Friedel, J. (1969). The Physics of Metals, in Ziman, J. M. (Editor), Cambridge University Press, Cambridge, pp 494.
25. Harrison, W. A., (1980), Electronic structure and properties of solids. The physics of chemical bonds. W. H. Freeman and company, San Francisco, Pp 200- 344.